



## COB-2021-1224

# NUMERICAL STUDY AND DEVELOPMENT OF AN EXPERIMENTAL TEST-RIG CONFIGURATION OF A SUPERSONIC NOZZLE FOR GAS SEPARATION

**Rodrigo Fazioli Gastaldo<sup>1</sup>**

**Julián Camilo Restrepo Lozano<sup>2</sup>, M.Sc.**

SISEA - Renewable and Alternative Energy Systems Laboratory, Mechanical Engineering Department, Escola Politécnica, University of São Paulo, São Paulo, SP, Brazil.

<sup>1</sup>r.gastaldo@aluno.ufabc.edu.br, <sup>2</sup>restrepo@usp.br

**Ricardo Galdino da Silva, PhD.**

Aeronautics and Space Institute - IAE, Aerodynamics Division, Department of Science and Aerospace Technology, DCTA, São José dos Campos, SP, Brazil.

ri\_galdino@yahoo.com.br

**Reinaldo Marcondes Orselli, PhD.**

Dept. Aerospace Engineering - Federal University of ABC, São Bernardo do Campo, SP, Brazil.

reinaldo.orselli@ufabc.edu.br

**José Roberto Simões Moreira, PhD.**

SISEA - Renewable and Alternative Energy Systems Laboratory, Mechanical Engineering Department, Escola Politécnica, University of São Paulo, São Paulo, SP, Brazil.

jrsimoes@usp.br

**Bruno Souza Carmo, PhD.**

Mechanical Engineering Department, Escola Politécnica, University of São Paulo, São Paulo, SP, Brazil.

bruno.carmo@usp.br

**Abstract.** *One of the challenges in exploration and extraction of natural gas is the large amount of carbon dioxide (CO<sub>2</sub>) present in the gas right after extraction. In that scenario, devices for gas separation have been developed, among which stands out the supersonic separator where its main advantage over others is to be compact and efficient, especially for large proportions of CO<sub>2</sub>. In this context and due to the device complex phenomena (high-speed compressible flow, non-homogeneous condensation, and two-phase swirling flow), the construction of a high-pressure experimental test-rig is required for the validation of numerical codes. This research contributes through the realization of three-dimensional numerical simulations based on a supersonic nozzle configuration for gas separation as a preliminary prototype to be used in experimental testing (based on the test-rig design), particularly with pressure measurements along the nozzle, vorticity distribution and shock wave flow visualization. Through the numerical results provided, the flow features, as aforementioned, along the configuration of the supersonic convergent-divergent nozzle are investigated. The Finite Volume Method is used for the numerical simulations. As the flow is highly turbulent, the flow governing equations (RANS) with turbulence modeling are applied. In addition, according to the operational range of the experimental tests, different outlet pressures, concentration of CO<sub>2</sub>, and nozzle pressure ratio are considered for the numerical investigation. Following that, by analyzing the flow characteristics along the preliminary prototype nozzle configuration, a modification is proposed in order to mitigate effects such as flow separation, boundary layer thickening and energy loss, thus contributing to the development of the test-rig by reducing the uncertainties of the measures in the experimental tests.*

**Keywords:** *supersonic separator, Computational Fluid Dynamics, turbulence modeling, shock wave.*

## 1. INTRODUCTION

Natural gas in Brazil, ANP (2020), stands out mainly in its use for thermal energy generation and industrial segments (petrochemical and fertilizer) and other more common uses like in vehicles, commerce, services and household, has the lowest carbon emission per KJ of energy produced among fossil fuels and sources such as natural and charcoal, which makes its use very convenient. According to the Brazilian Decennial Energy Expansion Plan, EPE (2019), the forecast for

2029 is that the Campos dos Santos basins will correspond to approximately 84% of the production of associated natural gas in Brazil and 195% growth in national natural gas production.

This increase in offshore natural gas exploration brings a challenge which is how to extract contaminants present in the raw gas mixture. According to ANP, the composition of natural gas is mostly methane (CH<sub>4</sub>), followed by ethane (C<sub>2</sub>H<sub>6</sub>) and, to a lesser extent, propane (C<sub>3</sub>H<sub>8</sub>). However, after extracting the raw gas from the fields, the presence of CO<sub>2</sub> can reach up to 70%, Imaev *et al.* (2014), so that large amounts of CO<sub>2</sub> must be separated and, this excess CO<sub>2</sub> can be reinjected into the fields or stored.

In this context of increase in natural gas production, a device capable of quickly and efficiently separating CO<sub>2</sub> as well as other impurities is in high demand. Techniques such as the one based on membrane permeation are indicated to deal with high levels of CO<sub>2</sub>. However, in the case of extractions carried out in offshore fields, they end up occupying too much space, becoming outdated. So, a compact device such as a supersonic separator has a great applicability potential, being capable of separating undesirable components such as CO<sub>2</sub>, H<sub>2</sub>S and water in a satisfactory manner from the hydrocarbons.

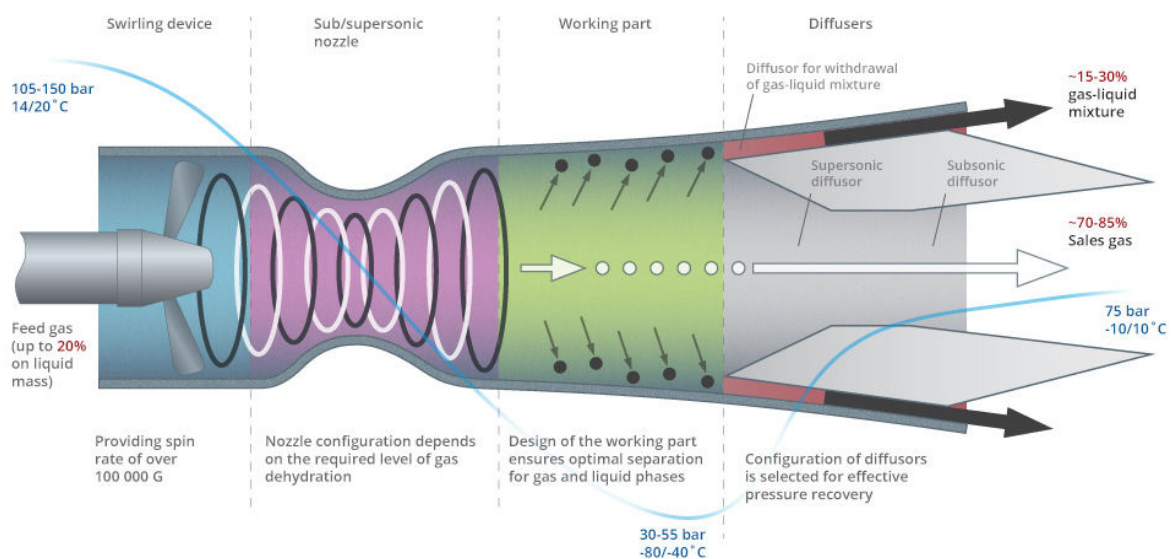


Figure 1. Basic scheme of 3S-separator by ENGO Engineering Ltd. (2016).

The supersonic separator schematized in Fig. 1, is a compact device, with a low operational cost and no moving parts. Liu *et al.* (2014) and Arinelli *et al.* (2015) described this technology. The separation is carried out by a convergent-divergent nozzle in which the gas is accelerated and captured by a collector. In the convergent-divergent nozzle, the gas is accelerated undergoing supersonic expansions, as result, the temperatures drops and causes the condensation of heavier components. In turn, the application of swirling flow allows the heavier condensed components to be brought to the inner walls of the device where collectors are well positioned to capture and separate these components from the rest of the gas.

## 2. OBJECTIVE

The present research proposal has as main objective to contribute through numerical simulations with the development of different test-rig configurations to be proposed in experimental tests of the supersonic separator. The proposed experiments will be carried out on the Polytechnic School facilities, mechanical engineering department, with funding from the RCGI (Research Center for Gas Innovation).

Numerical simulations are performed based on the configurations proposed by the experimental team of the RCGI research project for different experimental flow conditions. Several aspects are considered in the simulation, such as the preliminary geometry of the test-rig setup itself, evaluating points of separation of the flow, the thickness of the boundary layer and other characteristics of the flow that may affect the quality of the experiment to be carried out. Furthermore, modifications of the initial proposed geometries can be proposed and more detailed analyzes of the flow behavior of the different cases can be carried out. Further on, the results of the experiments can be compared to the respective results predicted by the numerical simulation, allowing an evaluation of the methodology used for the numerical simulations.

Three-dimensional geometries are considered in the simulations according to the configurations of the respective proposed experimental tests. In addition, the effect of ideal gas due to high pressure and multicomponent gas (in particular air and N<sub>2</sub> with CO<sub>2</sub> mixture) is analyzed. Finally different boundary conditions in the Outlet Static Pressure is analyzed.

### 3. METHODOLOGY

The numerical analysis of the test-rig channel starts by developing an unstructured three-dimensional mesh in ANSYS ICEM, Ansys, Inc. (2016), software for the prototype using the multi block-tool. The initial meshing process is focusing on refinement in high pressure gradient regions and a low-cost numerical analyses as the purpose of this research concerns to a qualitative study of the flow separation, turbulence generation downstream and thickening of the boundary layer.

The simulations are performed by ANSYS Fluent, Ansys, Inc. (2019), and Metacomp Technologies CFD++, Metacomp Technologies (2020), softwares. The software regarding the discretization of the computational domain is based on the Finite Volume Method, theory is described in Vesteeg and Malalasekera (2007). To deal with turbulent flow, the two-equation turbulence model  $k-\epsilon$  RNG, Yakhot *et al.* (1992), is used throughout the work (the RANS turbulence model is described in, Vesteeg and Malalasekera (2007), which is based on the original work of Yakhot *et al.* (1992)).

To deal with the compressibility effects of the flow due to the high Mach number (in the range 1.0-2.0 at the supersonic flow region), the numerical algorithms used are based on the model described in the Maliska (2017), a segregated solver algorithm adapted to deal with compressible flow.

Variations in the fluid, air, as an ideal gas to a real gas mixture (50%  $CO_2$ , 50%  $N_2$  - concentration) that incorporates the state equation in the methodology is also presented and compared. For a better representation of the problem, the Redlich-Kwong real gas model, Redlich and Kwong (1949), is used since it is capable of handling critical temperatures and high pressure gradients.

Further on, the post-processing of the results obtained in the numerical codes is carried on ANSYS EnSight, International, Inc. (2013). Finally a variation in the outlet static pressure as an objective to identify the shock wave position is conducted.

### 4. RESULTS AND DISCUSSION

#### 4.1 Geometry and mesh

##### 4.1.1 The experimental test-rig

Due to the device complex phenomena (high-speed compressible flow, non-homogeneous condensation), the construction of a high-pressure experimental test-rig is required for the validation of numerical codes. This test-rig must be designed to avoid flow detachment and to reduce uncertainties on the experimental tests. Fig. 2 presents the test-rig and nozzle design.

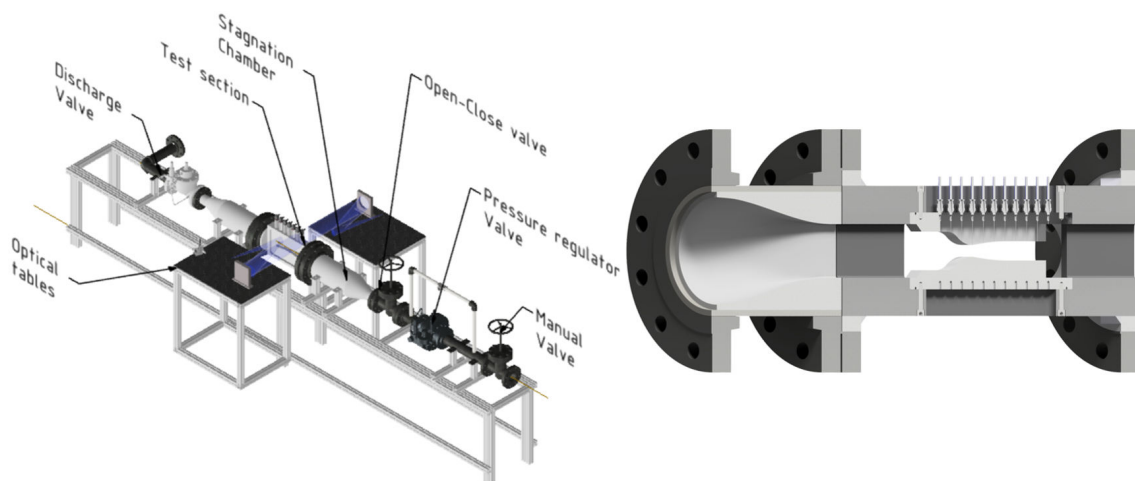


Figure 2. Experimental test-rig (left) and supersonic nozzle (Right). Carmo *et al.* (2020)

The nozzle channel is composed of a 3D adapter and a convergent-divergent nozzle, the nozzle was designed using the method of characteristic to avoid the formation of oblique shock waves within the nozzle. The test-rig is composed of pressure regulation valves for the control of the nozzle's inlet and outlet pressure and an optical table. The experimental test-rig may be used to test gas mixtures at different concentrations, pressures and temperatures, to emulate operation conditions in offshore platforms and, therefore, giving adequate diagnosis and feedback about the separator behavior. For its main experimental purpose, the use of optical methods for the flow diagnosis in complement with high-velocity data acquisition for high pressures and mass fractions will be used.

### 4.1.2 Mesh generation

As a non-axisymmetric geometry, the meshing process is done in the ANSYS ICEM CFD using the multi-blockage tool with one-quarter of the three-dimensional channel due to symmetry. The meshing generation process gave priority to carry out qualitative analysis of the flow behavior through the nozzle vis-à-vis the development and evaluation of the experimental geometry. The non-dimensional distance of the first cell adjacent to the wall ( $Y^+$ ) along the channel is based on the logarithmic law of the wall and as shown in Fig. 3 reached an interval of 0 to 235.4. Views of the mesh are represented in Fig. 4 and Fig. 5.

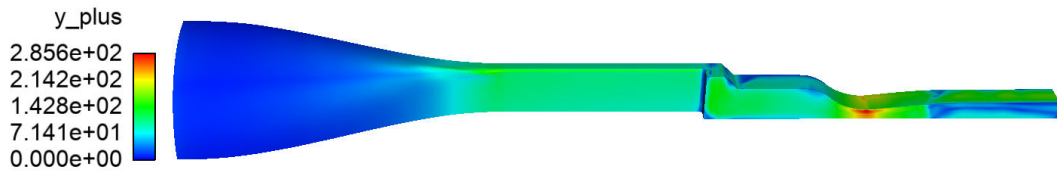


Figure 3.  $Y^+$  variation along the test-rig wall.

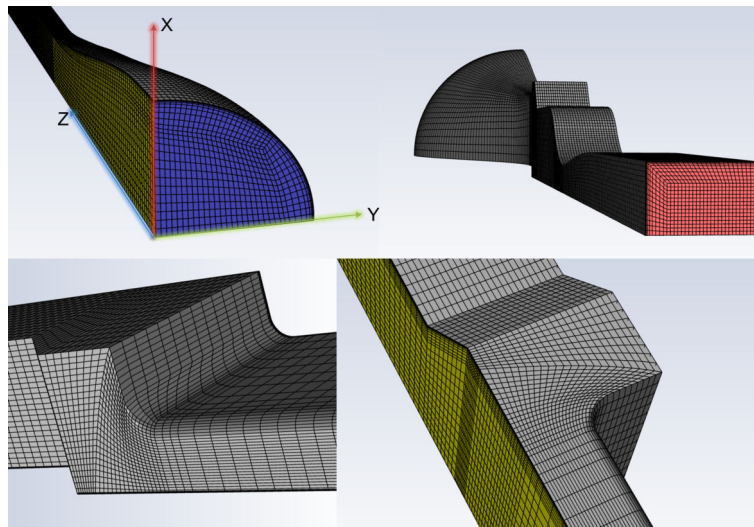


Figure 4. Mesh overviews.

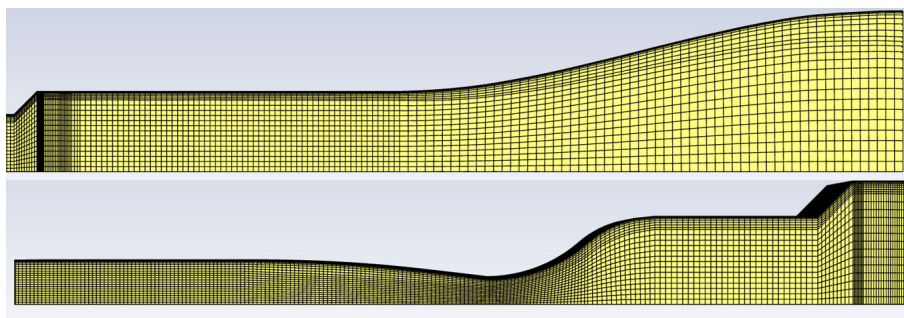


Figure 5. Mesh view: plane ZY

## 4.2 CFD code summary

### 4.2.1 Boundary conditions

Based on the experimental operating conditions for the test-rig, the boundary conditions of the numerical simulations are sititized in Tab. 1. The fluid used is air as an idea-gas, using the Sutherland, Ansys, Inc. (2019), variation for the viscosity.

Table 1. Boundary conditions for the first prototype, Outlet Pressure variation (4e5 Pa and 15e5Pa).

	Static Pressure	Total Pressure	Total Temperature	Hidraulic Diameter
<b>Inlet</b>	3.498e6 Pa	3.5e6 Pa	300 K	0.140 m
<b>Outlet</b>	4e5Pa and 15e5 Pa	-	300 K	0.031 m

The convergence criteria employed, as a general reference to both numerical codes, is the simulation to reach at least a residual value below 1e-3 for all transport equations, and below 1e-6 for the energy transport equation.

#### 4.2.2 Fluent numerical methodology

According to the segregated pressure-based solver, ANSYS Fluent is applied to deal with the pressure-velocity coupling in the three-dimensional simulations, solution method known as Couple, Ansys, Inc. (2019). This method allows the code to solve momentum and continuity equations together resulting in a better numerical convergence. The second-order upwind accuracy for the spacial discretization scheme is applied for all convective terms of the transport equations, Barth and Jespersen (1989), and the diffusive terms are discretized by a central differencing scheme, Vesteeg and Malalasekera (2007). The Pressure Staggering Option, Ansys, Inc. (2019), algorithm is applied, which is an interpolation scheme based on a 'staggered' control volume arrangement to compute the face values of pressure from the cell values.

#### 4.2.3 CFD++ numerical methodology

The code CFD++, Metacomp Technologies (2020), is a numerical CFD (Computational Fluid Dynamics) code developed and commercialized by Metacomp Technologies. For the present work, the CFD++ is set to use a compressible form of the Reynolds-Averaged Navier-Stokes equations (RANS) with the Realizable  $k - \epsilon$ , Chakravarthy *et al.* (2001), turbulence model as a closer model. In addition, the fluid (air), is assumed as a ideal gas. The CFD solver uses the finite volumes method for unstructured mesh. A Harten, Lax Van Leer with Contact wave (HLLC) Riemann, Perroomian *et al.* (1998), solver are used to define the (slop-limited) upwind fluxes. Moreover, the code uses second-order Total Variation Diminishing (TVD), Harten (1983), discretization based on a multi-dimensional interpolation.

#### 4.3 First prototype numerical results

According to the residual criteria used in this work, for the ideal gas simulations, Tab. 2, Fluent simulation did not reach the criteria for minimum residual as well as CFD++ in energy equation, k and Epsilon terms. In the real gas simulations with gas mixture, Tab. 3, only the 4 bar outlet pressure case achieved the criteria for the transport equations. Residuals of  $N_2$  in the 4e5 Pa and 15e5 Pa gas mixture case is, respectively, 2.1148e-16 and 1.5506e-06.

Table 2. Residual results with ideal air gas in both employed softwares.

Outlet Pressure	Continuity	x-velocity	y-velocity	z-velocity	Energy	k	Epsilon	
<b>Fluent</b>	4bar	1.3482e-03	4.4860e-05	5.4107e-05	1.1236e-04	5.2040e-06	1.2508e-03	9.4753e-04
	15bar	7.0936e-03	2.9377e-04	3.7830e-04	1.0117e-03	1.1061e-04	1.5582e-02	3.3573e-02
<b>CFD++</b>	4bar	3.4852e-04	4.0585e-04	1.2576e-05	2.3442e-04	1.1711e-02	5.2778e-01	1.1591e+00
	15bar	1.8084e-05	1.9808e-05	8.5010e-06	1.5436e-04	3.3748e-04	3.4767e+00	1.6782e+00

Table 3. Residual results with real gas mixture in Fluent.

Outlet Pressure	Continuity	x-velocity	y-velocity	z-velocity	Energy	k	Epsilon	
<b>Fluent</b>	4bar	9.4730e-04	3.8081e-05	4.2965e-05	9.6472e-05	3.3788e-06	1.1438e-03	1.0221e-03
	15bar	6.2952e-03	2.6085e-04	2.6094e-04	8.5355e-04	9.6122e-05	7.6630e-03	2.1058e-02

##### 4.3.1 Mach Number and Pressure

A normal shock wave occurs with high pressure gradients. Following the shock wave, flow separation occurs and reduction in velocity is identified after the strong adverse pressure caused by the sudden increase of pressure. In the current analysis (Outlet Pressure equal to 4e5 Pa) any normal shock wave have been developed. In this isentropic case the velocity increase until it reaches supersonic speeds in the convergence section after the adapter, now as a supersonic flow, there is a high acceleration in the fluid with the increase in the sectional area of the nozzle, reaching, after the throat,

values over Mach 2.00. As a result of Mach number increasing along the test-rig, the pressure decays. Figures 6 and 7 show this flow development.

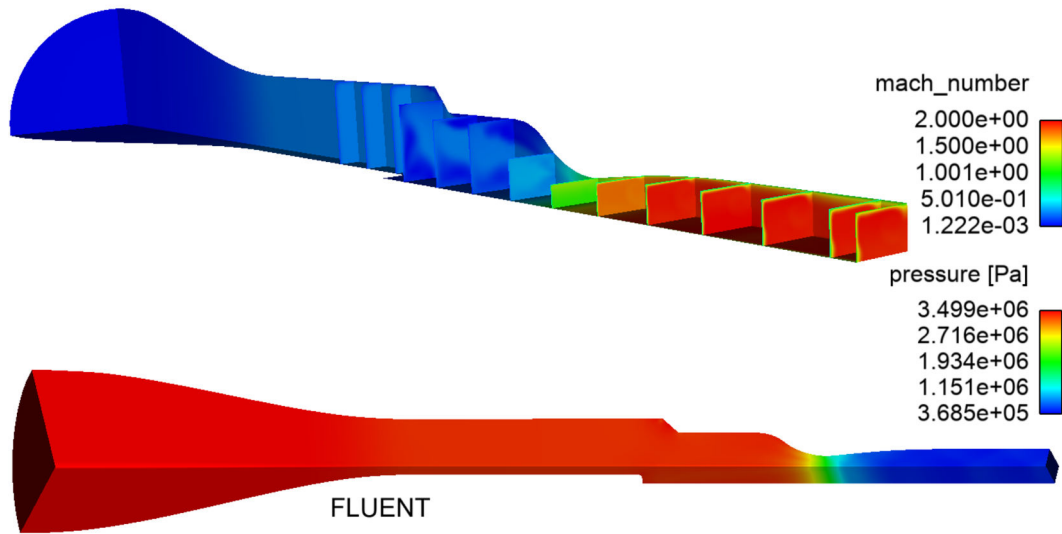


Figure 6. Mach Number [M] and Static Pressure [Pa], outlet pressure =  $4e5$  Pa.

The Fluent and CFD++ codes results are in close agreement, variations in the range of Mach number does not surpass an variation of 1.43%. Both cases did not develop a shock wave as seen in Fig. 7.

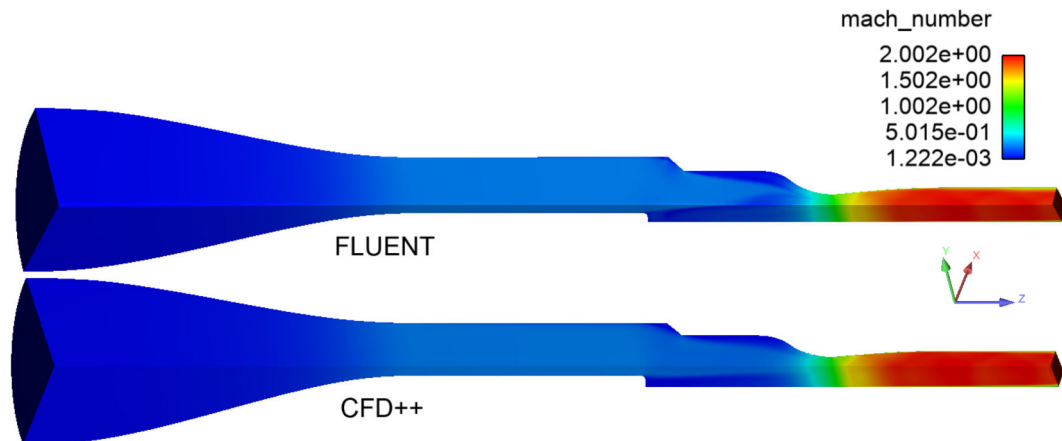


Figure 7. Mach number field comparison between Fluent and CFD++, outlet pressure =  $4e5$  Pa.

#### 4.3.2 Vorticity Magnitude

The vorticity magnitude is employed with a maximum range of  $5e3$  (1/s) for better visualization of the turbulence and wall detachment, considered important weight variables for the performance of test-rig experiments like flow visualization by the optical equipment and wall pressure data acquisition by transducers. Figure 8 shows the increase thickening of the boundary layer in the nozzle adapter as the fluid travels through the channel.

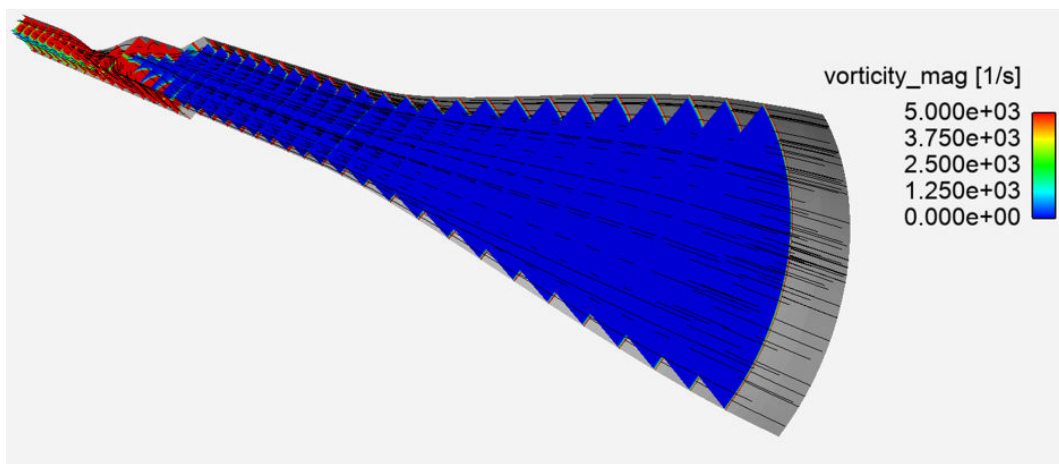


Figure 8. Overall view through the nozzle inlet section: Vorticity Magnitude (1/s) and Velocity Particle Streamlines, Outlet Pressure =  $4e5$  Pa.

As pointed in Fig. 9 and highlighted in Fig. 10, flow separations are visualized at the end of the adapter (beginning of the planar nozzle), which occur due to an abrupt increase in channel traversal area and the existence of surface corners. The flow detachment that occurs downstream the increase in width of the channel is more significant since the flow detachment generated by this change propagates downstream the throat and reaches the channel outlet.

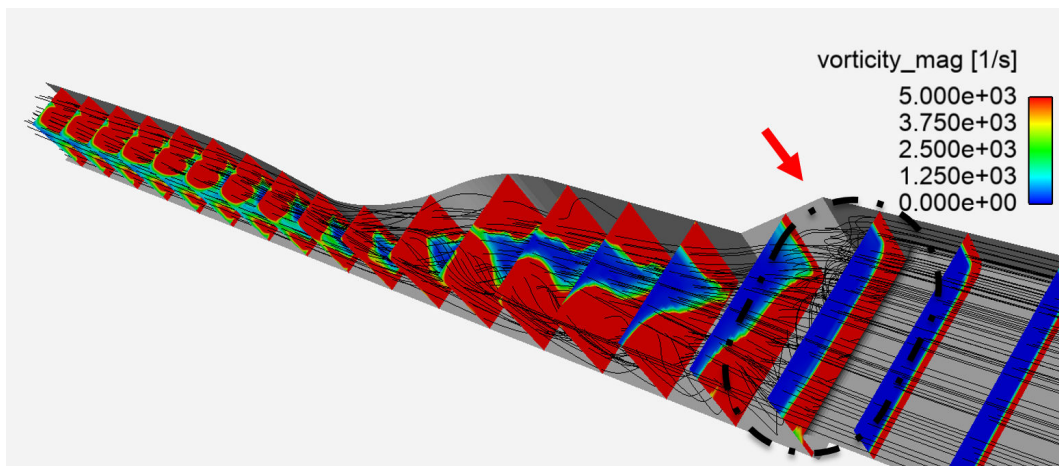


Figure 9. Overall nozzle view: Vorticity Magnitude (1/s) and Velocity Particle Streamlines, Outlet Pressure =  $4e5$  Pa.

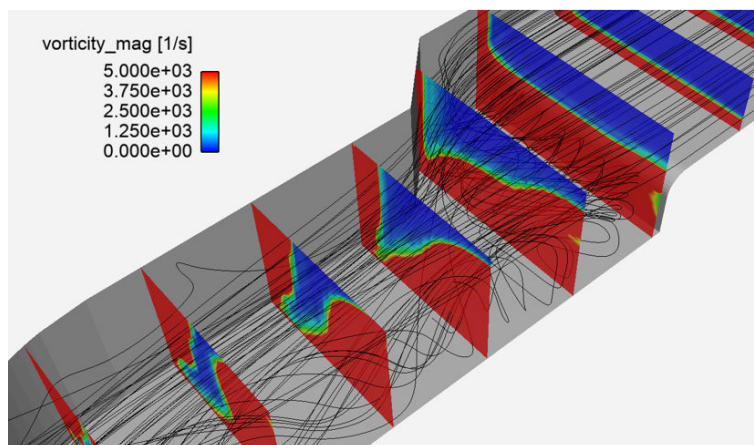


Figure 10. Adapter view: Vorticity Magnitude (1/s) and Velocity Particle Streamlines, Outlet Pressure =  $4e5$  Pa.

Figure 10 highlights the high recirculation that the junction adapter-nozzle creates with its abrupt increase in transversal area. Such recirculation which is carried downstream (as shown in Fig. 11) may possibly affect the quality of the

experiment at the end of nozzle section, thus a modification of the junction geometry may be proposed to mitigate this effect.

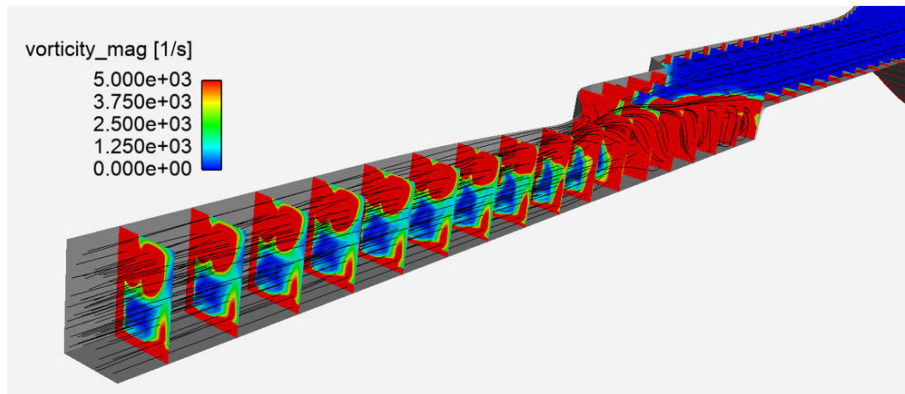


Figure 11. Divergent nozzle view: Vorticity Magnitude (1/s) and Velocity Particle Streamlines, Outlet Pressure =  $4e5$  Pa.

### 4.3.3 Outlet Pressure variation

Different experimental conditions will be tested with the test-rig which may cause the position of the shock wave vary between the throat and the outlet section. In one case is desirable that the shock wave occurs in the middle of the divergent part allowing visualizations and data acquisition using optical equipments, for other experimental purposes, it should occur close to the outlet section, ensuring that the flow reaches the reservoir in subsonic velocities. Thus outlet pressure of 15 bar is set to verify the position of the shock wave and the flow behavior for such flow conditions.

A variation in the value of the Outlet Pressure was set in order to find the best experimental condition of operation. Values between  $4e5$  Pa and  $15e5$  Pa was required to identify where the normal shock wave would appear, since the desirable place indicated was near the outlet nozzle diffuser, the following analysis have been conducted, see Fig. 12 and 13.

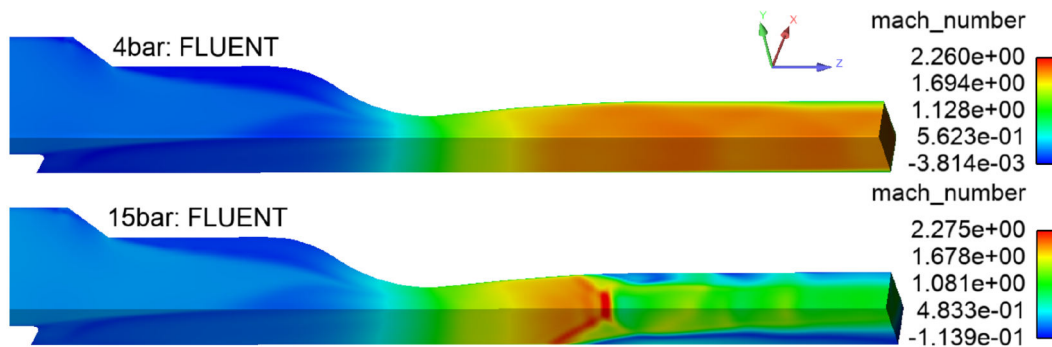


Figure 12. Mach Number overviews for Outlet Pressure variation in FLUENT.

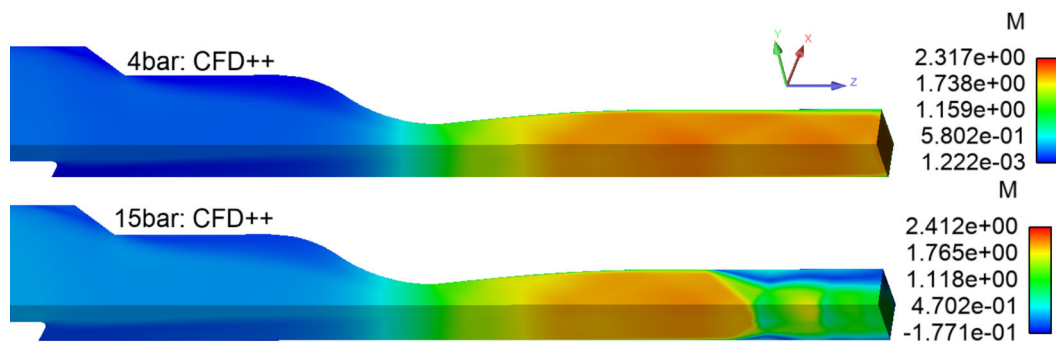


Figure 13. Mach Number overviews for Outlet Pressure variation in CFD++.

A normal shock wave is identified in the Outlet Pressure equal to  $15e5$  Pa case, with high pressure gradients, it is characterized with a lambda shape topology towards the wall due to its interaction with the nearby boundary layer. Both numerical codes simulations shown in Fig. 12 and 13 exhibit the shock wave.

The residual values obtained with the 15e5 Pa of Outlet Pressure did not reach the residual criteria for the current work as shown in Tab. 2. The high wall detachment, turbulence generated downstream the adapter and the formation of a sharp normal shock wave in the middle of the nozzle impacted this residual numbers.

Although the high residual numbers obtained, the results with 4e5 Pa and 15e5 Pa are consistent with what is expected according to the convergent-divergent nozzle theory. Future numerical analysis should verify if the use of the outlet diffuser as part of the simulating geometry could establish a better residual and give more precision to predict the best Outlet Pressure in function of the shock wave position and formation.

#### 4.3.4 Gas mixture

For a more accurate representation of the test-rig experiments, simulations with real gas (50%  $CO_2$ , 50%  $N_2$  - concentration) mixture are conducted in ANSYS Fluent considering the same turbulence model, boundary conditions and mesh as with the monocomponent gas case. As show in Fig. 14, the Mach number field does not show any substantial variations being compared with previous case (Fig. 12). With regard to the flow vorticity field and velocity streamlines shown in Fig. 15, the high recirculation, due to the abrupt increase in transversal area that the junction adapter-nozzle creates, remains being carried downstream the nozzle.

These similar results are expected as the Specific Heat Ratio ( $k$ ) of air ( $k = 1.4$ ) is close to the gas mixture employed in the experiments ( $k = 1.34$ ).

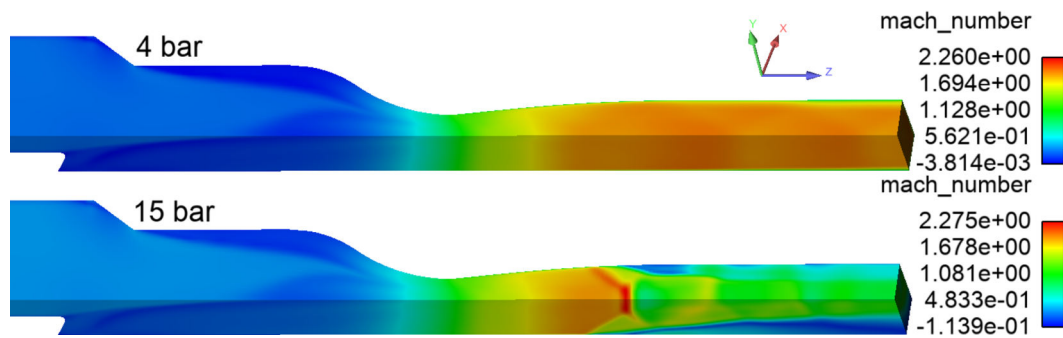


Figure 14. Mach Number overviews for Outlet Pressure variation in Fluent.

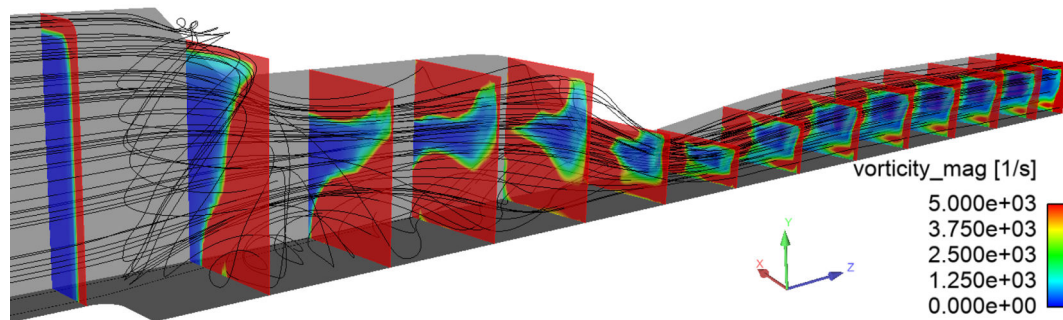


Figure 15. Overall nozzle view: Vorticity Magnitude (1/s) and Velocity Particle Streamlines, Outlet Pressure = 4e5 Pa.

## 5. CONCLUSION

In general, flow separation was identified right after the junction adapter-nozzle where an abrupt increase in the channel transversal area and surface corners is located. From this finding, it is recommended that the geometries of corners and adapters, where there are significant flow separations, as identified in Fig. 9 and 11, to be modified so as to mitigate such effects, and thus allowing a better quality of the experimental measurements to be carried out along the supersonic section (downstream the throat). In addition, due to proximity between the Specific Heat Ratio of both gases employed in this work, the simulations with the gas mixture that is used in the experimental tests showed similar results compared with the monocomponent case.

## 6. ACKNOWLEDGEMENTS

We gratefully acknowledge support of the RCGI – Research Centre for Gas Innovation, hosted by the University of São Paulo (USP) and sponsored by FAPESP – São Paulo Research Foundation (2014/50279-4) and Shell Brasil, and the strategic importance of the support given by ANP (Brazil’s National Oil, Natural Gas and Biofuels Agency) through the R&D levy regulation.

## 7. REFERENCES

- ANP, 2020. “Natural gas (in portuguese)”. Federal government. National Agency for Petroleum, Natural Gas And Biofuels. <http://www.anp.gov.br/gas-natural>. Accessed 10 August 2020.
- Ansys, Inc., 2016. “Ansys icem cfd user’s manual”.
- Ansys, Inc., 2019. “Ansys fluent theory guide”.
- Arinelli, L.O., Medeiros, J.L. and Araújo, O.Q., 2015. “Performance analysis and comparison of membrane permeation versus supersonic separator for co<sub>2</sub>”. *Offshore technology conference, OTC-26164-MS, Brazil, Rio de Janeiro-RJ, 27-29 October*.
- Barth, T.J. and Jespersen, D.C., 1989. “The design and application of upwind schemes on unstructured meshes”. *AIAA Paper 89-0366*.
- Carmo, B., Orselli, R., Galdino, R., Volpe, E., Cato, A., Kavabata, L., Costa, U., Cavalcante, J., Hayashi, M., Silva, E., Yamabe, P., Simões-Moreira, J., Restrepo, J., Acosta, A., Avencini, B., Baxmann, I., R.Costa and Junior, D.G., 2020. “Development of gas supersonic separators - optimisation, numerical simulation and experiments”. Technical report, Universidade de São Paulo.
- Chakravarthy, S., Goldberg, U., Batten, P., Palaniswamy, S. and Perroomian, O., 2001. “Some recent progress in practical cfd”. *AIAA Paper 2001-0136*.
- EPE, 2019. “2029 ten-year energy expansion plan (in portuguese)”. Federal government. Energy Research Company (EPE). Ministry of Mines and Energy, Brasília, <https://www.epe.gov.br/pt/publicacoes-dados-abertos/publicacoes/plano-decenal-de-expansao-de-energia-2029>. Accessed 10 August 2020.
- Harten, A., 1983. “High resolution schemes for hyperbolic conservation laws”. *J. Comput. Phys.*, 49 (2): 357–393, doi:10.1016/0021-9991(83)90136-5, hdl:2060/19830002586.
- Imaev, S.Z., Bagirov, L.A., Borisov, V.E. and Voytenkov, E.V., 2014. “New low temperature process of co<sub>2</sub> recovery from natural gases”. *SPE 171427, SPE Asia Pacific Oil Gas Conference and Exhibition, Adelaide, Australia*.
- International, Inc., C.E., 2013. “Ensign user manual for version 10.2”.
- Liu, X., Liu, Z. and Li, Y., 2014. “Investigation on separation efficiency in supersonic separator with gas-droplet flow based on dpm approach”. *Separation Science and Technology*, 49: 2603–2612.
- Ltd., E.E., 2016. “3s-technology: A brief description”. <http://www.engo3s.com/3s-tehnology>. Accessed 10 May 2021.
- Maliska, C.R., 2017. *Heat Transfer and Computational Fluid Mechanics (in portuguese)*. Grupo Gen-LTC.
- Metacomp Technologies, I., 2020. “Cfd++ user manual”. Agoura Hill CA.
- Perroomian, O., Chakravarthy, S., Palaniswamy, S. and Goldberg, U., 1998. “Convergence acceleration for unified-grid formulation using preconditioned implicit relaxation”. *AIAA Paper 98-0116, Reno, NV, Jan*.
- Redlich, O. and Kwong, J.N., 1949. “On the thermodynamics of solutions. v. an equation of state. fugacities of gaseous solutions.” *Chemical reviews*, Vol. 44, No. 1, pp. 233–244.
- Vesteeq, H.K. and Malalasekera, W., 2007. *An introduction to computational fluid dynamics - the finite volume method*. [S.l.]: Addison-Wesley-Longman.
- Yakhot, V., Orszag, S.A., Thangam, S., Gatski, T.B. and Speziale, C.G., 1992. “Development of turbulence models for shear flows by a double expansion technique”. *Physics of Fluids A*, Vol. 4, No. 7, pp1510-1520.

## 8. RESPONSIBILITY NOTICE

The authors are solely responsible for the printed material included in this paper.